

Prediction of the Second Transition Point of Tool Wear Phase Using Vibratory Signal Analysis (Z-ROT)

1st Nur Adilla Kasim
Department of Mechanical Engineering
Politeknik Mukah
Sarawak, Malaysia
nur.adilla@pmu.edu.my

2nd Mohd Ghafran Mohamed
Department of Mechanical Engineering
Politeknik Mukah
Sarawak, Malaysia
mohd.ghafran@pmu.edu.my

3rd Mohd Zaki Bin Nuawi
Department of Mechanical and
Manufacturing Engineering
Universiti Kebangsaan Malaysia
Selangor, Malaysia
mzm@ukm.edu.my

Abstract—Early intervention to change worn cutting tool before its failure could avoid unexpected machine downtime. A mathematical based predictive model is employed to estimate early tool failure using vibratory signal. The statistical-based signal analysis technique as wear tracking analysis is applied in the predictive model to outline the data pattern concerning wear and number of cutting. The signal analysis based on the changes in the vibration signatures that captured from accelerometer during the milling operation throughout the tool life. A significant correlation between the tool flank wear and the statistical index has achieved. The tool life as a function of the acceleration amplitude of assimilated vibrations. Selected curve fitting equations are considered to decide the transition point between the steady state and failure region. The result shows a significant expectation of determining the second transition point with estimate value of 0.235mm below the rapid wear (<0.25mm). The accuracy, reliability and robustness of the predicted transition point were then parallel against another sensing elements where it predicts almost the same transition point. The de-termination of the second transition point will assist the preparation to anticipate the tool to be bro-ken. The results reflected that the model gives reasonable estimation of tool life and the transition points at which changes of the region transpire.

Keywords—Cutting Tool Wear, Signal Analysis, Z-rot, Piezofilm-Based Sensor, Vibration

I. INTRODUCTION

The variation in cutting condition influence and alters the momentary and unpredictable cutting dynamic process and thus affects the cutting tool condition and process stability. As vibration be-come the primary effect, cutting tool condition and machine tools ultimately pay the price with worn tool eventually fails and broken machines. A vibratory system in machining operations consist the machine tool, cutting tool, workpiece and cutting conditions create a complex dynamic behaviour [1]. Vibration signals are one of the most widely analysed because they provide a thorough in-sight into the metal cutting process and considerably less complex in nature, more inclusive, and convenient [2]. The metal cutting process naturally produces vibration signal apart from mechanical vibration harvest from the tool wear and the cutting conditions

such as breakage [3]. Many researchers present vibration analysis for tool condition monitoring. Dimla and Lister [4] found that vibration signal is most tool wear sensitive to measure vibration signals in time and frequency domain analysis to predict tool wear. Chen et al. [5], Wang et al. [6], Elangoyan et al. [7], Rao et al. [8] and Rajesh and Namboothi [9] used vibration signals to measure reliability and wear correlation. Therefore make a prediction and develop tool condition monitoring successfully comply with selected method respectively. Recently, Aghdam et al. [10] captured wear sensitive features and derived from autoregressive moving average (ARMA) model of the recorded signals. The outputs of ARMA metric can also be used to provide reliable predictions for the tool.

The determination of transition point between mild and severe wear was the starting point. Mild wear is considered as acceptable wear state whereas the transition to severe conditions often represents a change to commercially unacceptable situations [11]. Therefore, the wear map was developed [12]–[15]. The well-known tool wear progression in machining describe the flank wear versus cutting time. The wear initially increases rapidly and later on gradually reduces to a constant rate until tool failure is reached. The wear rate was almost constant where there was no obvious transition from the steady-state in the failure region [16]. The point between the steady-state and failure region is known as the second transition point, STP.

Significant changes in the tool wear rate indicate the position of the transition time between the states. The values of the maximum wear corresponding to the first and second transition times are considered as the wear state criteria. The first and second criteria were found to be in the range of 0.05 – 0.1mm and 0.15 – 1.00mm, respectively, depending on the type of the operation [17]. Previous researchers have classified flank wear into three conditions in their tool wear monitoring studies using different analyses such as using wavelet analysis [18], fuzzy logic [19] and neural networks [20]. It consists of Phase 1 flank wear (VB = 0 - 0.15mm) were classified as a normal phase. Phase 2 flank wear (VB = 0.15 - 0.25mm), classified as medium abnormal phase. Lastly, phase 3 flank wear (VB = 0.25 - 0.30mm), classified as critical abnormal

phase. The three-period curve of flank face wear value increases from the initial wear (normal phase), and the wear rate is kept at a high level. It is followed by the steady normal wear (medium abnormal phase), where the wear rate is decreased. When the rapid wear takes place, the wear rate is the highest compared with the initial and normal periods, and therefore, the cutting stability is low. Based on the phenomenon, the ideal tool life should be before the rapid wear [21] where the wear value maximum of 0.250mm where STP is located. These works have been carried out to develop a more favourable tool wear tracking using vibration signals and eventually to predict and estimate the second transition point from the steady-state region into the failure region in tool wear monitoring. Until this paper is written, there is no specific and well-established method to determine the STP. This paper is offering an alternative way by using the previous developed statistical analysis to track the severity of wear index. The index then become input to the sequence of two lower order of polynomials in search for the second intersection point that resemble the STP in tool wear phase.

II. MATERIALS AND METHOD

An innovative, integrated rotating dynamometer was designed and constructed by Rizal to measure the cutting force in a wireless environment system [22]. This dynamometer utilised strain gauge that is mounted on legged cross beam transducer to measure three components of cutting force based on a rotating cutting force system as in Figure 1. Namely, main cutting force, F_c , thrust force, F_t and perpendicular cutting force, F_{cn} . Meanwhile an accelerometer, a thermocouple and strain gauge to measure torque are also built to the rotating dynamometer to build a multi sensor system.

This sensor system is then used for tool wear monitoring in milling P20+Ni tool steel using end milling cutting tool insert was tungsten carbide with multi-layer PVD TiAlN/AlCrN grade ACP200 (Code: AXMT170504PEER-G). A milling process experimental is prepared with various 2^3 full factorial combinations of cutting speed (200 and 373 m/min), feed rate (0.10 and 0.20 mm/tooth), radial depth of cut (0.4 and 0.6 mm) and axial depth of cut is kept constant at 1mm.

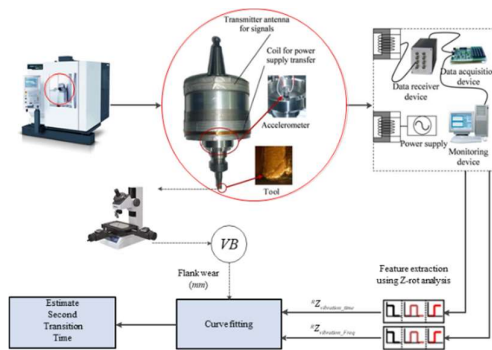


Fig. 1. Experimental setup

III. STATISTICAL ANALYSIS METHOD

The analysis produces Z-rot index as an input parameter that employs mathematical and statistical features (mean, standard deviation and Kurtosis) from signal data (such as force signal and vibration) [23]. The development of Z-rot predictive model (ZrPM) starts with the Z-rot tracking analysis method. Afterwards, ZrPM is determined to resolve

the unclear transition point from the second region to the third region. The transition point will be assessed to several-underlined curve fit-ting accordingly. The algorithm is summarized as presented in Figure 1.

A. Z-rotation Method

The selected features are suggested to among the best features to study wear correlation with signal amplitude [24]. It is based on a signal element variance scattering around its mean centroid. The method exhibits data pattern in defining the randomness of data features over the whole lifetime to diagnose inferences and expected to have more sensitivity toward amplitude and anomalies changes in a signal. These interpretations are beneficial for prediction and decision making such as in machine learning adaptation. It is also expected to be able to improve the wear progression curve which was unable to exhibit the three typical wear region for the cutting speed more than 120m/min [25]. Compute the distance, r , for each data variable by subtracting the mean data, \overline{sig}_y , from the data variable, sig_y to generate a zero-mean distribution [23].

$$r = (sig_y - \overline{sig}_y) \quad (1)$$

Based on the standard deviation and kurtosis value obtained, will gives the index, Z-rot, that indicates the current condition and records the wear evolution of cutting tool wear during the cutting process [23].

$${}^R Z = \frac{1}{N} \sqrt{\sigma_r^4 K_r} \quad (2)$$

Z-rot is a tracking analysis kurtosis-based use to track the severity of wear. It is expected to show a healthy relationship over the wear evolution.

B. Z-rot predictive model (ZrPM)

Several numbers of complex damage phenomena are happening within these stages (steady state and failure region) and require better understanding. The events are the likelihood to produce different wear progression scenarios. The wear progression scenario is significantly essential to predict the length (time) and propagation rate of each stage to predict the second transition point of a remaining lifetime as depicted in Figure 2.

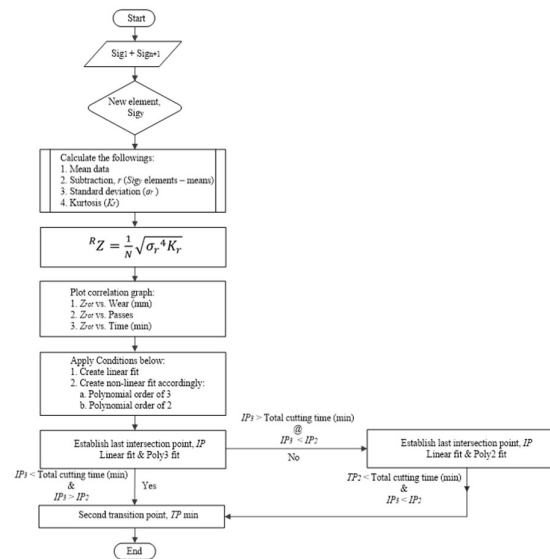


Fig. 2. Flowchart of the Z-rot predictive model (ZrPM)

The first attempt in spotting the time of the second transition point (TP_{STP}), plot a linear fit (Eq. 3) on the scattered data points followed by 2nd (Eq. 4) and 3rd (Eq. 5) order of polynomial regressions to fit the trend line:

$$f(x) = a_1x + a_0 \quad (3)$$

$$g(x) = a_2x^2 + a_1x + a_0 \quad (4)$$

$$h(x) = a_3x^3 + a_2x^2 + a_1x + a_0 \quad (5)$$

The decision to decide over the TP_{STP} is determining by the last intersection point between the linear and one of both polynomial regressions. The intersection point should not be extended too far outside the data. The choice is according to conditions:

- At first, consider the last intersection point (TP₃) between linear fit and the 3rd order of the polynomial. The intersection point must be within or under the total cutting time ($T_{Total\ cutting\ time}$) and has a bigger value from the other resulting last intersection point (TP₂) between the linear and 2nd order of the polynomial. The expression as stated:

$$TP_3 < \max(T_{Total\ cutting}) \ \&\& \ TP_3 > TP_2 \quad (6)$$

- If the intersection point does not comply either one or both conditions above, the system will return to consider the TP₂ resulted from crossing point between the linear and 2nd order of the polynomial.

$$TP_2 < \max(T_{Total\ cutting}) \quad (7)$$

IV. RESULTS AND DISCUSSION

A. Vibration Signal

Figure 3 and Figure 4 shows the time domain and frequency domain of vibration accelerations of the cutting process detected during the advancement of tool wear. It can be seen that dominant frequency activities occur at relatively low and middle-frequency regions. The high-frequency activities occur at low-frequency regions covering up to 500Hz and contain the most condition indicating information about the cutting process.

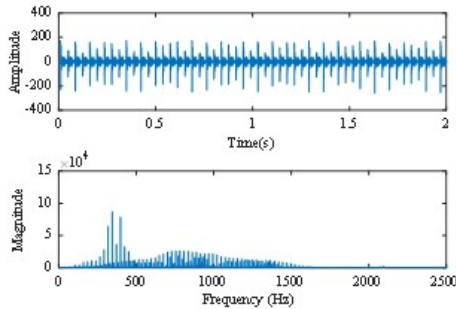


Fig. 3. Representative examples of Time domain and FFT analysis for the cutting vibrations ($v = 200\text{m/min}$, $f = 0.1\text{mm}$ and $d = 0.6\text{mm}$) for experiment 2 run 1

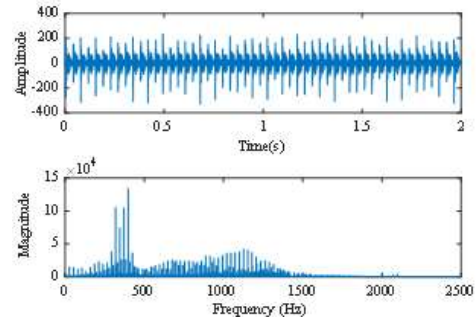


Fig. 4. Representative examples of Time domain and FFT analysis for the cutting vibrations ($v = 200\text{m/min}$, $f = 0.1\text{mm}$ and $d = 0.6\text{mm}$) for experiment 2 run 23

The magnitudes are also gradually increased with the advancement of tool wear and notably increased when the flank wear as in Fig. 3 has significantly developed from 0.001mm (run 1) to 0.131mm (run 23). The other frequency activities take place around after 500Hz up to 1500Hz which is the reflection of the damped natural frequency of the tool-workpiece system [26]. It can be seen in all experimental sets that characteristics of the frequency components located at the high-frequency region change with the advancement of wear. They occupy a larger frequency span around range between 500Hz and 1500Hz and their amplitudes rise when the severity of wear is increased.

B. Flank Wear Response

Figure 5 illustrates the statistic (Z-rot index) of the detected vibration acceleration signals at the mentioned cutting condition concerning the wear. During the very early phase of wear development, the amplitude of the vibration acceleration is slightly increased which is correspondingly reflected by the Z-rot. However, it is sometimes reduced when the wear starts developing on the tool's cutting edges which is also indicated as reductions in the Z-rot index as well as in signal amplitude. Nevertheless, the amplitudes of the ensuing Z-rot are then gradually increased with the advancement of wear where amplitude variations are also observed in the frequency domain. When the wear is fully developed over the flank surfaces at the end of wear test, the amplitude of the vibration signal magnitude represented by Z-rot index is notably increased, and the symptoms of tool wear are favorably revealed in the vibration signal plotting alongside with other sensors related. Estimation the Second Transition Point (STP)

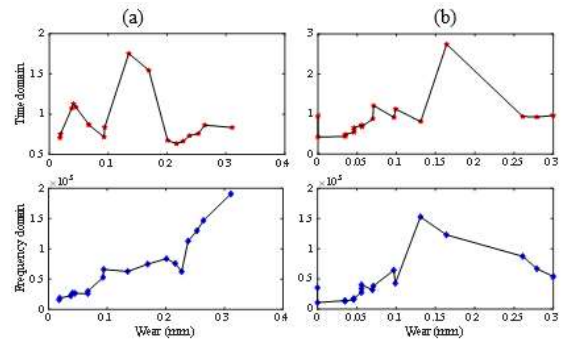


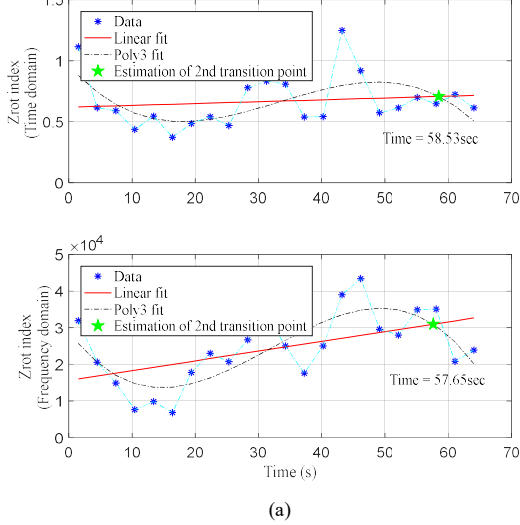
Fig. 5. Z-rot index of the vibration accelerations magnitude of cutting process during the advancement of wear: a) Experimental set 5 – $v = 375\text{m/min}$, $f = 0.1\text{mm}$, $d = 0.4\text{mm}$. b) Experimental set 6 – $v = 375\text{m/min}$, $f = 0.1\text{mm}$, $d = 0.6\text{mm}$.

C. Estimation of the Second Transition Point (STP)

The index was plotted using MATLAB software to see the variation within a certain time. The results of the machining tests and the analyses were portrayed together on the same graph for comparison and better understanding. The tool wear mechanisms trending is presented in figure 6.

Flank wear is the major failure pattern regardless the cutting speed. However, the tool wear is more critical at 375m/min compared with that at 200m/min. It is difficult to express the failure numerically, and therefore, the data are hard to collect within the limited experiments, resulting in that the rake face wear is out of the consideration of tool life evaluation in this case. The example of every last intersection point between linear and the polynomial regression fitting respectively of Z-rot vs cutting time are shown in Figure 4. In the time domain and frequency domain extracted of an experiment set 1, the second transition point is achieved at about 58.53s and 57.65s (approximate wear VB = 0.250mm) separately before the tool begins to total failure. While, with different speed level, the second transition point is considered around 15.82s and 14.4s (approximate wear VB = 0.250mm).

Vibration signal analysis for experimental set 1: v = 200m/min, f = 0.1mm, d = 0.4mm



Vibration signal analysis for experimental set 8: v = 375m/min, f = 0.2mm, d = 0.6mm

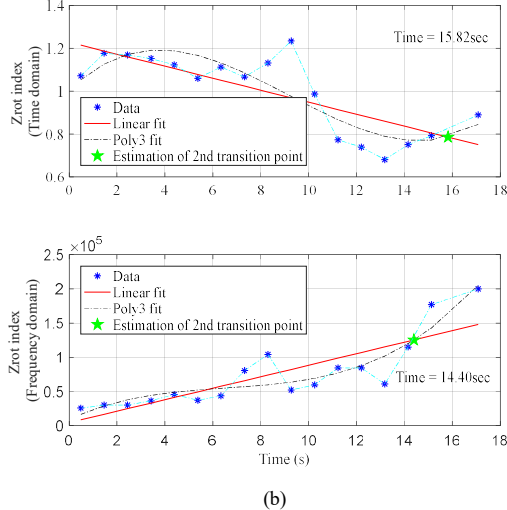


Fig. 6. Z-rot index progression for two experiment conditions and the fittings of polynomial regression of 2nd order and 3rd order

Both experiment condition was assigned to the maximum fit of 3rd order of the polynomial. As the 2nd order of polynomial would be detecting the STP earlier than what 3rd order of polynomial has. Comparing with the cutting speed 200m/min, the time to reach second transition point wear rate is faster at 375m/min approximately after 15s, and the wear value reaches the wear criterion rapidly after 17second. The overall result arrangement is in Table I.

D. The Relationship Between Vibration and Cutting Force

The signal data is analyzed in time domain using Z-rot analysis and the illustration as in Figure 7.

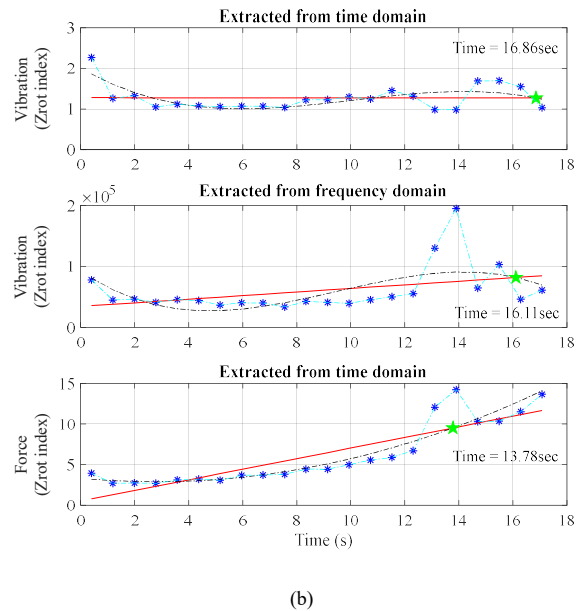
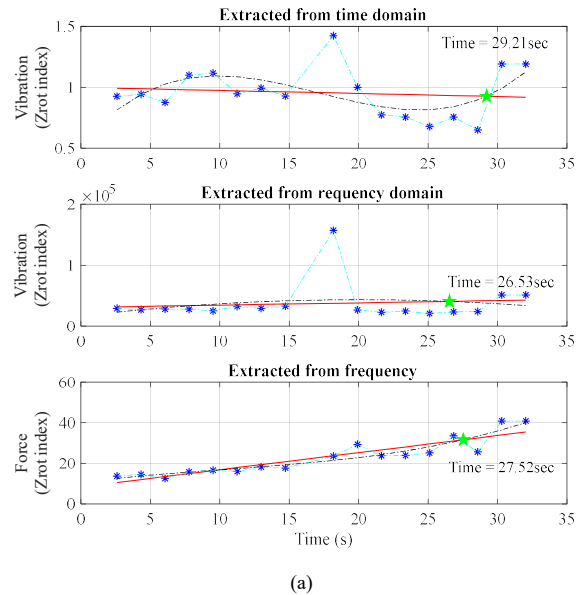


Fig. 7. a) Experimental set 4 - v = 200m/min, f = 0.2mm, d = 0.6mm. b) Experimental set 7 - v = 375m/min, f = 0.2mm, d = 0.4mm

Result validation of the model for estimating the transition times between the second and third states using vibration signal data, Z-rot prediction method also done on force signal data extracted simultaneously from the same experimental set.

The force signal data contain three components of cutting force based on a rotating cutting force system.

From the example observations and analyses made in Figure 7, it is clear that the cutting vibrations do not necessarily have the same varying pattern as that of the cutting forces in machining with either a sharp tool or a worn tool. In machining with a sharp tool and with a worn tool, the cutting forces can be very close to each of experimental sets, but the vibration magnitude can be very different. In addition, larger cutting forces do not necessarily lead to larger vibration amplitudes. For example, Figure 5b shows the time domain resultant force in Z-rot index in machining with a sharp tool is higher than that in time domain Z-rot index for vibration acceleration. In summary, the cutting forces are determined by material property, tool geometry, the cutting conditions, and so on. The cutting forces not only determine the cutting vibration, but also by the structural rigidity (such as damping and stiffness) of the tool-work-machine system [27].

E. Overall Estimation of the Second Transition Point

The outline of the overall result to estimate STP for the various condition, different sensors signal data (vibration, force components and torque) where vibration both in the time domain and in frequency domain while force and torque were analysed in time domain respectively as in Table I.

TABLE I. OVERALL ESTIMATION OF THE SECOND TRANSITION POINTS FOR VARIOUS MACHINING CONDITION

Set	Total cutting time (s)	Predicted STP of Average	Set
1	64.06	56.71	~ 0.210
2	64.06	52.02	~ 0.230
3	32.03	27.08	~ 0.210
4	32.03	28.05	~ 0.240
5	34.16	30.66	~ 0.250
6	34.16	28.79	~ 0.240
7	17.08	15.57	~ 0.250
8	17.08	15.53	~ 0.250

Based on the observation made above, the predicted STP values are mostly similar at certain machining conditions. The predicted second transition point has an average of predicted wear 0.235mm as the ideal tool life should be before the rapid wear [22] as the maximum wear land width (VB) at steady state region is 0.250mm. The new statistical feature, Z-rot index have been carried out to as characteristic feature for tool wear tracking using vibration signals and eventually, ZrPM was able to predict and estimate the second transition point from the steady-state region into the failure region in tool wear monitoring.

V. CONCLUSION

The resulting trend of the Z-rot index analysis is useful in determining the second transition point in wear phase. Using vibration signal, ZrPM identified the specific safe cutting time in every test sample. The method is proposed as an alternative autonomous technique to monitor cutting tool wear progression during the machining process. ZrPM is time savvy and successful for observing the tool wear phase and avoiding traditional direct tool wear observation.

REFERENCES

- [1] G. H. Lim, "Tool-wear monitoring in machine turning," *J. Mater. Process. Technol.*, vol. 51, no. 1-4, pp. 25-36.
- [2] M. S. H. Bhuiyan, I. A. Choudhury, and Y. Nukman, "Tool Condition Monitoring using Acoustic Emission and Vibration Signature in Turning," in *Proceedings of the World Congress on Engineering 2012 Vol III WCE 2012, July 4 - 6, 2012, London, U.K., 2012.*
- [3] D. E. Dimla, "Sensor signals for tool-wear monitoring in metal cutting operations—a review of methods," *Int. J. Mach. Tools Manuf.*, vol. 40, no. 8, pp. 1073-1098, Jun. 2000, doi: 10.1016/S0890-6955(99)00122-4.
- [4] D. E. Dimla and P. M. Lister, "On-line metal cutting tool condition monitoring," *Int. J. Mach. Tools Manuf.*, vol. 40, no. 5, pp. 739-768, Apr. 2000, doi: 10.1016/S0890-6955(99)00084-X.
- [5] B. Chen, X. Chen, B. Li, Z. He, H. Cao, and G. Cai, "Reliability estimation for cutting tools based on logistic regression model using vibration signals," *Mech. Syst. Signal Process.*, vol. 255, pp. 2526-2537, 2011.
- [6] G. F. Wang, Y. W. Yang, Y. C. Zhang, and Q. L. Xie, "Vibration sensor based tool condition monitoring using support vector machine and locality preserving projection," *Sensors and Actuators*, vol. 209, pp. 24-32, 2015.
- [7] M. Elangovan, V. Sugumaran, and S. Ramachandran, K. i. Ravikumar, "Effect of SVM kernel functions on classification of vibration signals of a single point cutting tool," *Expert Syst. Appl.*, vol. 38, pp. 15202-15207, 2011.
- [8] K. V. Rao, B. S. N. Murthy, and N. M. Rao, "Cutting tool condition monitoring by analyzing surface roughness, work piece vibration and volume of metal removed for AISI 1040 steel in boring," *Measurement*, vol. 46, pp. 4075-4084, 2013.
- [9] V. G. Rajesh and V. N. N. Nambhothiri, "Flank wear detection of cutting tool inserts in turning operation: application of nonlinear time series analysis," *Soft Comput.*, vol. 14, pp. 913-919, 2010.
- [10] B. H. Aghdam, M. Vahdati, and H. M. Sadeghi, "Vibration-based estimation of tool major flank wear in a turning process using ARMA models," *Int J Adv Manuf Technol*, vol. 76, pp. 1631-1642, 2015.
- [11] J. A. Williams, "Wear modelling: analytical, computational and mapping: a continuum mechanics approach," *Wear*, vol. 225, pp. 1-17, 1999, doi: 10.1016/S0043-1648(99)00060-5.
- [12] S. . Lim, "Recent developments in wear-mechanism maps," *Tribol. Int.*, vol. 31, no. 1, pp. 87-97, 1998, doi: 10.1016/S0301-679X(98)00011-5.
- [13] M. F. Ashby and S. C. Lim, "Wear-mechanism maps," *Ser. Metall. Mater.*, vol. 24, no. 5, pp. 805-810, May 1990, doi: 10.1016/0956-716X(90)90116-X.
- [14] A. Cantizano, A. Carnicero, and G. Zavarise, "Numerical simulation of wear-mechanism maps," *Comput. Mater. Sci.*, vol. 25, no. 1, pp. 54-60, 2002, doi: 10.1016/S0927-0256(02)00249-5.
- [15] R. Bosman and D. J. Schipper, "Mild Wear Prediction of Boundary-Lubricated Contacts," *Tribol. Lett.*, vol. 42, no. 2, pp. 169-178, 2011, doi: 10.1007/s11249-011-9760-3.
- [16] H. Z. Li, H. Zeng, and X. Q. Chen, "An experimental study of tool wear and cutting force variation in the end milling of Inconel 718 with coated carbide inserts," *J. Mater. Process. Technol.*, vol. 180, no. 1, pp. 296-304, 2006, doi: 10.1016/j.jmatprotec.2006.07.009.
- [17] V. P. Astakhov, "The Assessment of Cutting Tool Wear," *Int. J. Mach. Tools Manuf*, vol. 44, no. 6, pp. 637-647, 2004.
- [18] K. Zhu, Y. S. Wong, and G. S. Hong, "Multi-category micro-milling tool wear monitoring with continuous hidden Markov models," *Mech. Syst. Signal Process.*, vol. 23, no. 2, pp. 547-560, Feb. 2009, doi: 10.1016/j.ymsp.2008.04.010.
- [19] G. Wang, L. Qian, and Z. Guo, "Continuous tool wear prediction based on Gaussian mixture regression model," *Int. J. Adv. Manuf. Technol.*, vol. 66, no. 9, pp. 1921-1929, 2013, doi: 10.1007/s00170-012-4470-z.
- [20] S. Cho, S. Binsaeid, and S. Asfour, "Design of multisensor fusion-based tool condition monitoring system in end milling," *Int. J. Adv. Manuf. Technol.*, vol. 46, no. 5, pp. 681-694, 2010, doi: 10.1007/s00170-009-2110-z.
- [21] W. Ji, J. Shi, X. Liu, L. Wang, and Steven Y. Liang, "A Novel Approach of Tool Wear Evaluation," *J. Manuf. Sci. Eng.*, vol. 139, 2017.

- [22] M. Rizal, J. A. Ghani, M. Z. Nuawi, and C. H. C. Haron, "A Wireless System and Embedded Sensors on Spindle Rotating Tool for Condition Monitoring," *Adv. Sci. Lett.*, vol. 20, no. 10–12, pp. 1829–1832, 2014.
- [23] N. A. Kasim, M. Nuawi, J. Ghani, M. Rizal, M. A. F. Ahmad, and C. Haron, "Cutting tool wear progression index via signal element variance," *J. Mech. Eng. Sci.*, vol. 13, pp. 4596–4612, 2019, doi: 10.15282/jmes.13.1.2019.17.0387_rfseq1.
- [24] P. Krishnakumar, K. Rameshkumar, and K. I. Ramachandran, "Tool Wear Condition Prediction Using Vibration Signals in High Speed Machining (HSM) of Titanium (Ti-6Al-4V) Alloy," *Procedia Comput. Sci.*, vol. 50, pp. 270–275, 2015, doi: 10.1016/j.procs.2015.04.049.
- [25] Z. M. Nuawi, F. Lamin, M. N. M. J., N. Jamaluddin, S. Abdullah, and E. N. C. K., "Integration of I-kaz Coefficient and Taylor Tool Life Curve for Tool Wear Progression Monitoring in Machining Process," *Int. J. Mech.*, vol. 1, no. 4, pp. 44–50, 2007.
- [26] I. Yesilyurt and H. Ozturk, "Tool condition monitoring in milling using vibration analysis," *Int. J. Prod. Res.*, vol. 45, no. 4, pp. 1013–1028, 2007.
- [27] N. Fang, P. S. Pai, and S. Mosquea, "A comparative study of sharp and round-edge tools in machining with built-up edge formation: cutting forces, cutting vibrations, and neural network modeling," *Int J Adv Manuf Technol*, vol. 53, pp. 899–910, 2011.